Čerenkov Emission of Quasiparallel Whistlers by Fast Electron Phase-Space Holes during Magnetic Reconnection

M. V. Goldman,[1,*] D. L. Newman,[1] G. Lapenta,[2] L. Andersson,[1] J. T. Gosling,[1] S. Eriksson,[1] S. Markidis,[3] J. P. Eastwood,[4] and R. Ergun[1]

[1]*University of Colorado, Boulder, Colorado 80309, USA*
[2]*Leuven Universiteit, Celestijnenlaan 200B, B-2001 Leuven, Belgium*
[3]*KTH Royal Institute of Technology, SE-100 44 Stockholm, Sweden*
[4]*The Blackett Laboratory, Imperial College London, SW7 2AZ London, United Kingdom*

(Received 24 September 2013; published 8 April 2014)

Kinetic simulations of magnetotail reconnection have revealed electromagnetic whistlers originating near the exhaust boundary and propagating into the inflow region. The whistler production mechanism is not a linear instability, but rather is Čerenkov emission of almost parallel whistlers from localized moving clumps of charge (finite-size quasiparticles) associated with nonlinear coherent electron phase space holes. Whistlers are strongly excited by holes without ever growing exponentially. In the simulation the whistlers are emitted in the source region from holes that accelerate down the magnetic separatrix towards the x line. The phase velocity of the whistlers v_φ in the source region is everywhere well matched to the hole velocity v_H as required by the Čerenkov condition. The simulation shows emission is most efficient near the theoretical maximum v_φ = half the electron Alfven speed, consistent with the new theoretical prediction that faster holes radiate more efficiently. While transferring energy to whistlers the holes lose coherence and dissipate over a few local ion inertial lengths. The whistlers, however, propagate to the x line and out over many 10's of ion inertial lengths into the inflow region of reconnection. As the whistlers pass near the x line they modulate the rate at which magnetic field lines reconnect.

DOI: 10.1103/PhysRevLett.112.145002 PACS numbers: 94.30.cp, 52.25.Os, 52.35.Hr, 52.35.Sb

Electromagnetic (EM) whistler waves are commonly found in space [1–4], and in laboratory experiments [5] and are often observed during magnetic reconnection [6–9]. Various kinetic electron distributions have been found which drive whistlers unstable. The most commonly cited unstable distributions are electron temperature anisotropy [10] and electron beams [11,12], although there are other unstable distributions [13]. The quasiparticle Čerenkov emission of EM whistler waves found in the reconnection simulations in this Letter via both simulation and theory is a fundamentally different physical mechanism, in which the whistlers do not exponentiate from noise, as in kinetic instabilities.

Quasiparticle Čerenkov emission [14] is an unusual process which can be understood simply in terms of an inhomogenous nonlinear current $\mathbf{J}_0$, in a spatially uniform background plasma. Let $\mathbf{J}_0(\xi_\parallel - v_0 t, \xi_\perp) = v_0 \rho_0(\xi_\parallel - v_0 t, \xi_\perp)$ represent a finite-sized spatial clump of coherent charge density ρ_0 moving at speed v_0 along a background magnetic field $\mathbf{B}_0$ in the spatial direction $\xi_{||}$. In its own frame $\rho_0(\xi_{||}, \xi_\perp)$ is assumed here to be the stationary charge density of a moving electron phase space hole, found from Poisson's equation in terms of the trapping potential whose parallel gradient is the bipolar electrostatic field associated with phase space holes. Such holes have been observed as bipolar parallel electrostatic field structures in space physics [15–17] for over 12 years. They are often associated with magnetic reconnection in magnetospheric [6,18] and laboratory plasmas [19].

The spatial transform of the finite-sized hole current is

$$\mathbf{J}_0(k_\parallel, k_\perp, t) = \mathbf{v}_0 \rho_0(k_\parallel, k_\perp) e^{ik_\parallel v_0 t}, \tag{1}$$

which, for a given $k_{||}$, oscillates at the Doppler frequency, $k_{||} v_0$. Resonant driving of a weakly damped wave with real frequency ω_w occurs if $\rho_0(k_{||})$ is appreciable for values of $k_{||}$ which satisfy the resonance condition, $k_{||c} v_0 = \omega_w(k_{||c})$. Note that the resonance condition is the same as the Čerenkov condition, $v_0 = \omega_w / k_\parallel$.

In the magnetotail reconnection simulations described in this Letter quasiparallel EM whistlers are found for the first time to be Čerenkov emitted by the current J_0 of holes moving down the magnetic separatrix towards the x line. The whistler phase velocity v_φ is clearly Čerenkov matched to the hole velocity v_H in the source region in the simulation. Emission is seen to be most efficient for v_H near the theoretical maximum $v_\varphi = v_{Ae}/2$, where $v_{Ae} = \sqrt{(B^2/4\pi n m_e)} = c\Omega_e/\omega_e$ is the electron Alfven speed. Here, B and n are the local magnetic field and density. This simulation result is consistent with a new theoretical prediction that holes with v_H near $v_{Ae}/2$ radiate more efficiently than slower holes.

The response of *damped* whistler waves with real frequency ω_w to J_0, is just like that of a *damped* harmonic oscillator to an external force resonantly oscillating at ω_w:

$$E(t) \propto J_0(1-e^{-\gamma t})\frac{\omega_w}{\gamma}, \qquad \lim_{t\ll\gamma^{-1}} E(t) \propto \omega_w t. \quad (2)$$

The current J_0 plays the role of external force. The whistler field E does not grow exponentially from noise as in the kinetic theory of linearly unstable plasma waves. In the steady state, E is proportional to the large factor ω_w/γ. The simulations in this Letter show that even for shorter times $t \ll \gamma^{-1}$ the whistler field $E \propto t$ experiences secular time dependence that enables it to become as large as the hole bipolar field, which loses coherence and dissipates over a few local ion inertial lengths. Meanwhile, the whistlers propagate over 10's of ion inertial lengths, influencing the reconnection rate and penetrating deeply into the inflow region.

The bipolar fields associated with the Čerenkov-emitting holes near the separatrix have been verified both by observation [18] and by PIC simulations [18,20–22]. Our simulations of magnetotail reconnection show that electrons are trapped by the potential created by an inhomogeneous two-stream electron instability, as will be discussed in a future publication. There are many other different ways to trap electrons, such as by Buneman instability near the x line in strong guide field simulations [23], by sheath potentials [13], and even electromagnetically, by the second-order Lorentz force of preexisting highly nonlinear whistlers [24]. None of these other processes is relevant here.

Hole quasiparticle Čerenkov emission of *electrostatic* waves (*not* whistlers) has been treated theoretically [14] in a strongly magnetized plasma, with $v_{Ae} > c$, but is not relevant to tail reconnection, in which $v_{Ae} < c$.

The implicit 2D particle-in-cell reconnection simulations used here are based on a code which has been published and vetted extensively [20–22,25]. The parameters employed in these simulations are appropriate to Earth's magnetotail and identical to those employed in our published simulations [26] and confirmed by others [27]. The electron temperature is $T_e = 1$ keV and $T_i = 5T_e$. The ion mass is $256m_e$. The initial condition is a Harris equilibrium with maximum density n_0 and background density $n_b = 0.1n_0$. The *local* electron inertial length $d_e = \Omega_e v_{Ae}$ at the location of the holes is well resolved. The grid spacing is around fifteen local electron Debye lengths, comparable to the size of holes observed by Themis [28]. The ratio of the speed of light c to the *initial Harris sheet* Alfven speed v_{A0} is $c/v_{A0} = 100$ and the electron thermal velocity is $v_e/c = 0.045$. The simulations have an out-of-plane guide field $Bg = 0.1B_0$ where B_0 is the asymptotic B_x. Although B_g is small, it makes the holes near the separatrix legs more robust and it leads to more efficient whistler emission from two of the four separatrix legs.

The simulation box size is $L_x \times L_y = 200d_{i0} \times 30d_{io}$, where d_{i0} is the Harris-density ion inertial length $d_{i0} = c/v_{A0}$, where, $v_{A0} = \sqrt{B_0^2/(4\pi n_0 M_i)}$. *Simulation coordinates* are used in which z is out of plane and y is orthogonal to x in the reconnection plane. Boundary conditions are periodic in $\pm x$ and conducting in $\pm y$. Reconnection is initiated by a small perturbation at $x = 100d_{io}$ that becomes an x point flanked by exhaust outflow and flux-pileup fronts moving away from it in $\pm x$.

Figure 1(a) shows the reconnection field $E_z(x, y)$ in the reconnection plane at time $\Omega_i t \approx 30$. Wave oscillations are evident in E_z, mainly moving left in the top inflow region and moving right in the bottom inflow region. An interpretation in terms of linear whistler waves in a uniform magnetized plasma is depicted by the arrows near one of the nominal *source regions* in the sketch insert in Fig. 1(a). The local quasistatic background (zero-order) magnetic field vector is **B**. The wave vector **k** has components antiparallel and perpendicular to **B**. The high-frequency electric and magnetic wave fields $\mathbf{E}_w$ and $\mathbf{B}_w$ are approximately right-circularly polarized (rotating in the direction of electrons).

Whistlers and bipolar fields in the $\{x\text{-}y\}$ reconnection plane are shown in Figs. 1(b),(c). The whistler waves are pronounced in Fig. 1(b)—a plot of $[\partial_t \mathbf{B}]_{\perp 1} \approx \partial_t \mathbf{B}_w$, where $\perp 1$ indicates the component of a vector perpendicular to **B**, and in the x-y plane. A nominal source region is displayed as a small rectangle between $x = 112.5d_{i0}$ and $117.5d_{i0}$. Both $E_{||}$ [Fig. 1(c)] and whistlers propagate down the separatrix from the vicinity of the source region, where the latter are initially weak. The whistlers gain amplitude, eventually leaving the separatrix to propagate along incoming flux tubes. Whistlers emanating from source regions near the *lower left* separatrix leg propagate towards the lower inflow region. Whistlers emanating from the other two separatrix legs are much weaker by the time they cross into the inflow region. (See movie in the Supplemental Material [29].)

As will be seen in Fig. 2, the bipolar fields in the whistler source region [shaded rectangle in Fig. 1(c)] accelerate down the separatrix, but, unlike the whistlers, the holes die out along the separatrix leg near $x \approx 110d_{i0}$. They are spatially correlated with the propagating whistlers that intensify as the holes fade. Figure 1(d) shows how bipolar fields in $E_{||}$ correspond to well-resolved phase-space holes in the source region. The electron distribution function is plotted in $\{x\text{-}v_{||}\}$ phase space, with x spanning the source region rectangle in Fig. 1(c). The line intersections in Fig. 1(d) mark the centers of two holes in the source region moving left with velocities $v_H \approx -15v_{A0} = -0.40v_{Ae}$ and $v_H \approx -18v_{A0} = -0.47v_{Ae}$. These are also the velocities of the corresponding bipolar fields and of the quasiparticles that emit whistlers. As a hole moves to the left, its speed $|v_H|$ increases.

The well-known theoretical cold-fluid plasma expression for the frequency of a wave on the whistler-electron-cyclotron branch with small perpendicular wave number is given in terms of local parameters by Eq. (3).

$$\varpi_w = \frac{q^2}{(1+q^2)}, \qquad u_\varphi = \frac{q}{(1+q^2)}, \qquad q \equiv k_{||} d_{eL}. \quad (3)$$

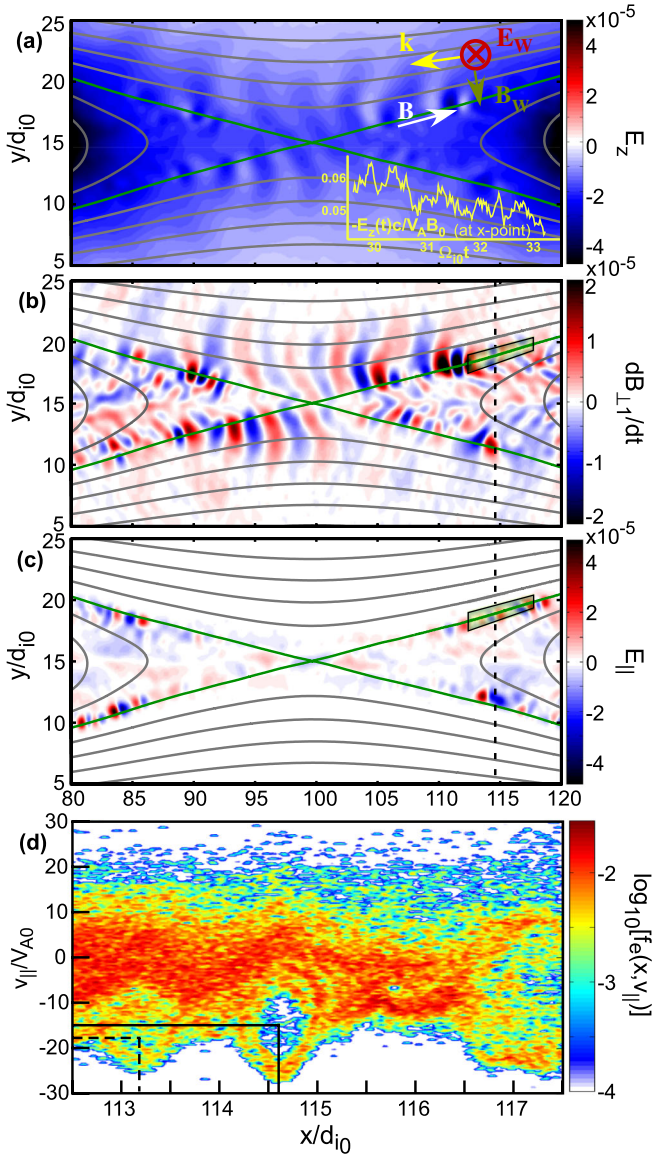

FIG. 1 (color online). (a) Reconnection field E_z at $\Omega_i t \approx 30$, shows whistlers emanating from separatrix (green). Sketch: idealized linear whistler. Inset: Reconnection rate as a function of time. (See the movie of E_z in the Supplemental Material [29]). (b) $[\partial t B]_{\perp 1}$ whistler waves, (c) $E_{||}$ bipolar structures near separatrix (green) at $\Omega_i t \approx 30$; Rectangle on upper right separatrix is nominal *source region*. (d) Electron $\{x\text{-}v_{||}\}$ phase space in source region showing two holes of different speeds.

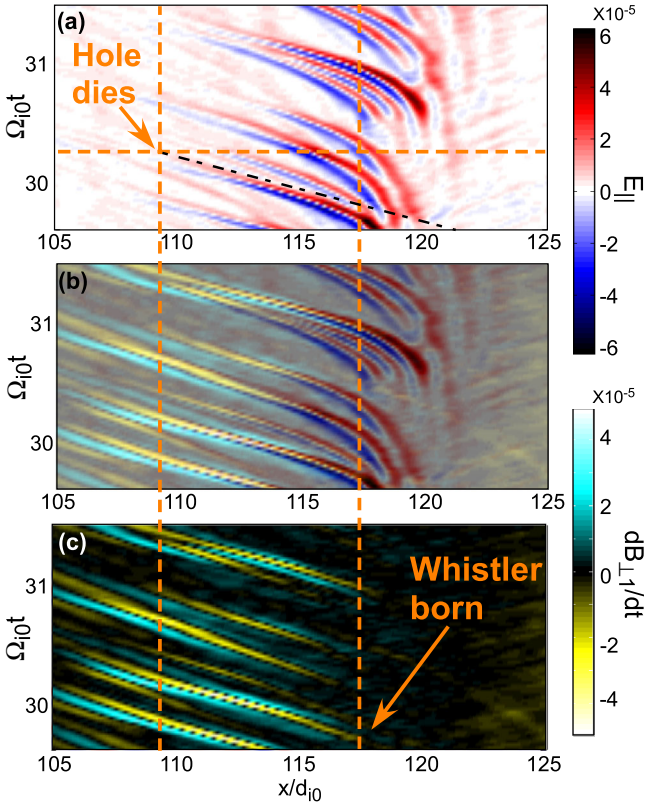

FIG. 2 (color online). $\{x\text{-}t\}$ time histories of bipolar fields $E_{||}$ in (a) and of whistlers, $[\partial_t B]_{\perp 1}$ in (c) and of both together in (b), showing whistlers Čerenkov emitted by holes.

The dimensionless whistler parallel wave number q is expressed in terms of the local electron inertial length d_{eL}. The dimensionless whistler frequency, $\varpi_w = \omega_w/\Omega_e$ is in terms of the local electron cyclotron frequency and the whistler phase velocity $u_\varphi = \varpi_w/q$ is naturally expressed as $u_\varphi = v_\varphi/v_{AeL}$, in terms of the local electron Alfvén speed, v_{Ae}.

Corrections to the whistler frequency in Eq. (3), due to the perpendicular wave number $k_\perp$, are small provided $(k_\perp/k_{||})^2 \ll 1$, a condition satisfied in the simulation. For $q = 1$, Eq. (3) yields $\varpi_w \approx 0.5$ and $u_\varphi \approx 0.5$—the maximum u_φ that a whistler can have under these conditions.

In both the inflow and source regions $B_x \approx 0.6 B_0$ and $n \approx n_0/16$, although there is considerable nonuniformity in the source region. Hence, locally, $\Omega_e \approx 0.6\Omega_{e0}$, $d_e \approx d_{i0}/4$, $v_{Ae} \approx 38 v_{A0}$, and $v_{Ae}/c \approx 0.38$.

From examination of the inflow region in Fig. (1), the approximate whistler parallel wavelength is $\lambda \approx 4 d_{i0}$, so, $k_{||} d_e \approx -0.39$ in the inflow region and Eq. (3) predicts a whistler with frequency $\varpi_w \approx 0.13$ and phase velocity $u_\varphi \approx -0.33$. These theoretical results in the inflow region are consistent with the frequency and phase velocity extracted from the simulation alone without using Eq. (3).

The time dependence of the reconnection electric field E_z at the x point is also influenced by whistlers. This means that the topological *reconnection rate* [shown in the inset in the lower right in Fig. 1(a)] is time-modulated by whistlers: The longer time scale ≈20% fluctuations in the reconnection rate with period $\Omega_{i0}\tau \approx 0.4$ corresponds to whistlers at the x point with frequency $\varpi_w \approx 0.1$

In the nominal *source region* the whistler phase velocity, frequency, and parallel wave number are all larger and will be found in terms of the hole velocity from the Čerenkov condition. Figure (2) shows the $\{x\text{-}t\}$ "time histories" of both the moving holes and whistlers in the source region

defined in Fig. (1). The three plots show $\mathbf{E}_\parallel$ [Fig. 2(a)], $[\partial_t \mathbf{B}]_{\perp 1}$ [Fig. 2(c)], and a combined plot of both Fig. 2(b) as functions of x and t, with $y = y(x)$ on the separatrix.

As seen in the $E_{||}$ time history, Fig. 2(a), the holes are born around $x \approx 119 - 120 d_{i0}$. They accelerate into the whistler source region, moving towards the x-line and expire at $x \leq 110 d_{i0}$. The emission lifetime of the hole in the yellow-shaded rectangle is $\Delta t \approx 0.7 \Omega_{i0}$. This is the difference between the time at which the hole expires and the time at which the whistler first appears. The slope of a bipolar field structure in Fig. 2(a) is the inverse velocity of the associated hole-quasiparticle. The slope of the structures in Fig. 2(c) gives the inverse phase velocity of whistlers. It is clear from Fig. 2(b) that v_H and $v_{\varphi x} \approx v_\varphi$ track each other smoothly at all times and locations *definitively verifying* the Čerenkov condition $v_H = v_\varphi$.

The dot-dashed slope in Fig. 2(a) yields $|u_H| = 0.47$ ($v_H \approx -18 v_{A0}$), an asymptotic hole velocity consistent with the same hole in Fig. 1(d) at an earlier time when it was slower ($v_H = -15 v_{A0}$, $u_H = 0.40$). For a given hole velocity, $u_H < 0.5$ there are two solutions to Eq. (3) for the whistler parallel wave number q in terms of the hole velocity $q_\pm = \eta \pm \sqrt{(\eta^2 - 1)}$, with $\eta \equiv 1/(2|u_H|)$. The whistlers corresponding to $|u_H| = 0.47$ have parallel wave numbers $q_- \approx 0.72$ and $q_+ \approx 1.4$, yielding frequencies both above and below [4] $\varpi_w \approx 0.5$.

The efficiency of the whistler emission in the source region over the emission lifetime of the hole can be estimated theoretically and compared with the value found from Fig. (2). The Fourier-transformed equations for linear waves with electric field $\mathbf{E}$ driven by $\mathbf{J}_0$ as described in the introduction takes the usual form, $\mathrm{M} \cdot \mathbf{E} = 4\pi i \mathbf{J}_0/\omega$, where M is the well-known Maxwell matrix [10], obtained from Maxwell's equations and the linearized cold fluid equations in a coordinate system of right-and left-circularly polarized and parallel electric field components $E_{R,L,z}$ given by Kennel [10]. Taking the inverse M^{-1} yields the electric field E_w of a right-circularly polarized whistler in terms of the hole current. It is assumed that $k_\perp = 0$ except in the matrix element $[\mathrm{M}^{-1}]_{R,z} \propto k_\perp$, which couples the z current $\mathbf{J}_0$ to the right-circularly polarized whistler field $\mathbf{E}_w$. The perpendicular wave number is needed in the *coupling* because EM Čerenkov emission requires a component of $\mathbf{J}_0$ parallel to $\mathbf{E}_w$, or $\mathbf{E}_w \cdot \mathbf{J}_0 \neq 0$.

A bi-Maxwellian model [14] of the shape of $J_0(\xi_{||}, \xi_\perp)$ is introduced in which a is the Gaussian half-width in the parallel direction $\xi_{||}$ and b is the half-width in the perpendicular direction $\xi_\perp$. From the inverse time transform of E_w the whistler electric field $E_w(q_\pm, k_\perp, t)$, can be expressed as a factor R times the hole electric field $E_H(k_{||}, k_\perp)$, which is proportional to $J_0(k_{||}, k_\perp)$ through Poisson's equation.

$$|E_H| = d_e \varphi_0 \tilde{a}\, \tilde{b}\, q_\pm \mathrm{Exp}\left\{ -(\tilde{a}^2 q_\pm^2 + \tilde{b}^2 q_\perp^2)/2 \right\}, \qquad (4a)$$

$$R = \left| \frac{E_w}{E_H} \right| = (t\Omega_e) \frac{2 v_{Ae}^2 u_H^4}{c^2} [q_\pm q_\perp], \qquad (4b)$$

As in Eq. (2), $E_w \propto t$ is *secular*. The dimensionless perpendicular wave number is defined as $q_\perp \equiv k_\perp d_e$. From the simulation [Fig. (2)], $\tilde{a} \equiv a/d_e \approx 1.5$, and $\tilde{b} \equiv b/d_e \approx 2.5$. The ratio $R = |E_w/E_H|$ is proportional to ${u_H}^4$, so holes radiate whistlers most efficiently at higher speeds, u_H, subject to $u_H \leq 1/2$. Because of the small guide field the holes on the upper right and lower left separatrix legs are generally faster than the holes on the lower right and upper left separatrix legs, which may explain why the latter don't radiate as efficiently.

Equation 4(b) can give an estimate of the time τ it takes for the whistler E_w to grow as large as the hole $E_{||}$. The time τ for R to reach 1 is $\Omega_{eL}\tau = c^2/(2 v_{AeL}^2 u_H^4 [q_\pm q_\perp]) \approx 55/[q_\pm q_\perp]$, after inserting $v_{AeL}/c = 0.38$, and $u_H \approx 0.5$. Next, estimate $[q_\pm q_\perp]$ as ≈ 0.3, which maximizes the product of $[q_\pm q_\perp]$ with the bi-Maxwellian form of $J_0(k_{||}, k_\perp)$ used in Eq. 4(a). More explicitly, $q_\perp \approx (1/\tilde{b}) = 0.4$ and $q_\pm = q_- = 0.72$, since the response at q_+ is suppressed by the $k_{||}$ dependence in $J_0(k_{||}, k_\perp)$. The emitted whistler frequency associated with $q_- = 0.72$ is $\omega_w = 0.36 \Omega_{eL}$, although a band of nearby frequencies will be emitted as the hole accelerates. A spectral analysis (not shown) displays just such a band of frequencies.

Hence, $\Omega_{eL}\tau \approx 183$, or, equivalently, $\Omega_{i0}\tau \approx 1.2$, which is within a factor of 2 of the hole emission life time, $\tau\Omega_{i0} \approx 0.7$, found in the simulation from Fig. 2.

The holes and whistlers therefore remain in contact with one another long enough for the whistlers to reach a significant amplitude ($E_w \approx E_H$), but not so long that the secular growth approximation breaks down. As in Eq. (2), the secular approximation is valid even for kinetically-*damped* whistlers for times $\tau \ll \gamma^{-1}$, where γ is the kinetic damping rate. Damping can thus be ignored as long as $2\gamma/\Omega_e \ll 0.01$. From the parallel phase space distribution in Fig. 1(d) it is clear that the part of the electron distribution function that supports the whistler is a flattop which falls off rapidly with $v_{||}$, thus yielding only very weak damping, estimated at $2\gamma/\Omega_{eL} \ll 10^{-2}$.

It has been shown from both theory and simulation that almost-parallel propagating whistlers are created by electron phase space holes moving sufficiently fast near separatrix legs in weak-guide-field magnetic reconnection. The holes act as moving quasiparticles which Čerenkov emit the whistlers. In the source region, the whistlers are emitted in a band of frequencies $<0.5\Omega_e$, with parallel wave numbers $k_{||} d_e < 1$, and with parallel phase velocity, $v_\varphi \approx v_{Ae}/2$, where v_{Ae} is the local *electron* Alfven speed. This phase velocity is also the hole velocity at which whistler emission is most efficient. The holes disintegrate as the whistlers grow and then penetrate deep into the

reconnection *inflow regions* where they have longer wavelengths and lower frequencies and phase velocities. Theory and simulation results for the whistler frequency and phase velocity are in good agreement both in the source and inflow regions. The efficiency of the emission process has been calculated theoretically and predicts a hole-whistler interaction time within a factor of 2 of the value found in the simulation.

Electron velocity-space plots in the *source region* reveal that $T_{e\perp} < T_{e||}$, so that electron temperature anisotropy instabilities cannot account for the whistlers emanating from the source region treated here, although they can be elsewhere [9].

These results can be significant for satellite detection of magnetic reconnection in the magnetotail. Assuming a physical electron mass, the simulation yields $E_{w-\max} \approx 20$ mV/m in the source region, comparable to the simulation bipolar field $E_{H-\max}$ and to the value of $E_{H-\max} = 50$ mV/m *measured* during tail reconnection [18]. From Faraday's law the whistler magnetic field corresponding to $E_{w-\max} \approx 20$ mV/m is $B_{w-\max} \approx 0.6$ nT. A measured [18] reconnection field, $B_0 = 30$ nT, and local density of $n_e = 0.08$/cc yield in the source region a hole size of $1.5d_e = 30$ km and a whistler frequency of $f_w = 420$ Hz. The predicted modulation of the reconnection rate is on the order of 20%, with frequency $f_w = 100$Hz typical of whistler frequencies in the inflow region. The electron Alfven speed is $v_{Ae} \approx 10^5$ km/s, so the fastest holes (at $v_{Ae}/2$) which theory and simulation predict to be the most efficient Čerenkov emitters of whistlers in the source region are too fast for Cluster to measure using time-delay methods.

The upcoming NASA-Magnetosphere Multiscale Mission (MMS) is designed to probe electron physics at high resolution. Electron physics includes electron holes, whistlers, and properties of the electron diffusion region during tail (and dayside) reconnection. The whistlers predicted here in the inflow region indicate proximity to an x-line and to the electron diffusion region. Together with electron holes, these whistlers will be part of the triggers for data selection on the FIELDS instrument on MMS [30]. Experimental verification of the correlation of emitting holes with emitted whistlers will be a challenge since the source region where holes and whistlers are both large enough to be seen simultaneously is small. However, MMS is designed to probe these small (electron) scales in more detail, thus presenting further opportunities to correlate source region whistlers with the bipolar fields associated with electron holes at the edge of the outflow exhaust and to look for modulation in the reconnection E field in the electron diffusion region near the x-line.

Thanks to Professor J. Drake for useful discussions. Work and computer simulations supported by NASA Grants No. NNX08AO84G and No. NNX12AG70G, and NASA computer resources.

*goldman@colorado.edu

[1] R. A. Helliwell, *Whistlers and Related Ionospheric Phenomena* (Stanford Univ. Press, Stanford, 1965).
[2] A. J. Kopf *et al.*, Geophys. Res. Lett. **37**, L09102 (2010).
[3] C. T. Russell, T. L. Zhang, M. Delva, W. Magnes, R. J. Strangeway, and H. Y. Wei, Nature (London) **450**, 661 (2007).
[4] W. Li, J. Bortnik, R. M. Thorne, C. M. Cully, L. Chen, V. Angelopoulos, Y. Nishimura, J. B. Tao, J. W. Bonnell, and O. LeContel, J. Geophys. Res. **118**, 1461 (2013).
[5] R. L. Stenzel, Phys. Rev. Lett. **38**, 394 (1977); J. M. Urrutia, C. L. Rousculp, and R. L. Stenzel, Solar System Plasmas in Space and Time, Geophys. Monograph **84**, 129 (1994).
[6] X. Tang, C. Cattell, J. Dombeck, L. Dai, L. B. Wilson, A. Breneman, and A. Hupach, Geophys. Res. Lett. **40**, 2884 (2013); CA. Cattell *et al.*, Geophys. Res. Lett. **29**, 1065 (2002).
[7] A. Vaivads, Geophys. Res. Lett. **31**, L03804 (2004).
[8] O. Le Contel *et al.*, Ann. Geophys. **27**, 2259 (2009).
[9] X. Deng, M. Ashour-Abdalla, M. Zhou, R. Walker, M. El-Alaoui, V. Angelopoulos, R. E. Ergun, and D. Schriver, J. Geophys. Res. **115**, A09225 (2010).
[10] C. F. Kennel and H. E. Petschek, J. Geophys. Res. **71**, 1 (1966); C. F. Kennel, Phys. Fluids **9**, 2190 (1966).
[11] T. F. Bell and O. Bunemann, Phys. Rev. **133**, A1300 (1964); K-I Nishikawa, O. Buneman, and T. Norbert, Geophys. Res. Lett., **21**, 1019 (1994).
[12] S. P. Gary, J. Geophys. Res. **90**, 10815 (1985).
[13] Z. Guo and X. Z. Tang, Phys. Rev. Lett. **109**, 135005 (2012).
[14] N. Singh, S. M. Loo, and B. E. Wells, Geophys. Res. Lett. **28**, 1371 (2001).
[15] R. Ergun, Y.-J. Su, L. Andersson, C. Carlson, J. McFadden, F. Mozer, D. Newman, M. Goldman, and R. Strangeway, Phys. Rev. Lett. **87**, 045003 (2001).
[16] J. R. Franz, J. Geophys. Res. **110**, A09212 (2005).
[17] M. V. Goldman, D. L. Newman, and A. Mangeney, Phys. Rev. Lett. **99**, 145002 (2007).
[18] C. Cattell, J. Geophys. Res. **110**, A01211 (2005).
[19] W. Fox, M. Porkolab, J. Egedal, N. Katz, and A. Le, Phys. Rev. Lett. **101**, 255003 (2008).
[20] G. Lapenta, S. Markidis, A. Divin, M. Goldman, and D. Newman, Phys. Plasmas **17**, 082106 (2010).
[21] S. Markidis, G. Lapenta, L. Bettarini, M. Goldman, D. Newman, and L. Andersson, J. Geophys. Res. **116**, A00K16 (2011).
[22] A. Divin, G. Lapenta, S. Markidis, D. L. Newman, and M. V. Goldman, Phys. Plasmas **19**, 042110 (2012).
[23] J. F. Drake, Science **299**, 873 (2003).
[24] Y. Katoh and Y. Omura, J. Geophys. Res. **111**, A12207 (2006).
[25] S. Markidis and G. Lapenta, Math. Comput. Simul. **80**, 1509 (2010).
[26] M. V. Goldman, G. Lapenta, D. L. Newman, S. Markidis, and H. Che, Phys. Rev. Lett., **107**, 135001 (2011).
[27] A. Le, J. Egedal, O. Ohia, W. Daughton, H. Karimabadi, and V. Lukin, Phys. Rev. Lett., **110**, 135004 (2013).
[28] J. B. Tao *et al.*, J. Geophys. Res. **116**, A11213 (2011).
[29] See Supplemental Material at http://link.aps.org/supplemental/10.1103/PhysRevLett.112.145002 for movie of whistler propagation.
[30] R. Ergun (private communication).